J. Math. Biol. (2015) 70:1645–1668
DOI 10.1007/s00285-014-0813-8

Mathematical Biology

A boundary-layer solution for flow at the soil-root interface

Gerardo Severino · Daniel M. Tartakovsky

Received: 17 July 2013 / Revised: 16 June 2014 / Published online: 10 July 2014

Abstract Transpiration, a process by which plants extract water from soil and transmit it to the atmosphere, is a vital (yet least quantified) component of the hydrological cycle. We propose a root-scale model of water uptake, which is based on first principles, i.e. employs the generally accepted Richards equation to describe water flow in partially saturated porous media (both in a root and the ambient soil) and makes no assumptions about the kinematic structure of flow in a root-soil continuum. Using the Gardner (exponential) constitutive relation to represent the relative hydraulic conductivities in the Richards equations and treating the root as a cylinder, we use a matched asymptotic expansion technique to derive approximate solutions for transpiration rate and the size of a plant capture zone. These solutions are valid for roots whose size is larger than the macroscopic capillary length of a host soil. For given hydraulic properties, the perturbation parameter used in our analysis relates a root's size to the macroscopic capillary length of the ambient soil. This parameter determines the width of a boundary layer surrounding the soil-root interface, within which flow is strictly horizontal (perpendicular to the root). Our analysis provides a theoretical justification for the standard root-scale cylindrical flow model of plant transpiration that imposes a number of kinematic constraints on water flow in a root-soil continuum.

G. Severino (✉)
Division of Water Resources Management and Bio-System Engineering, University of Naples, Federico II via Universitá 100, 80055 Portici, Naples, Italy
e-mail: severino@unina.it

D. M. Tartakovsky
Department of Mechanical and Aerospace Engineering, University of California, 9500 Gilman Drive EBU II, Mail Code 0411 La Jolla, San Diego, CA 92093, USA
e-mail: dmt@ucsd.edu

Keywords Plant transpiration · Water uptake · Rhizosphere · Singular perturbation · Matching asymptotic

Mathematics Subject Classification 76S05 · 92C80 · 34D15

1 Introduction

Transpiration is widely recognized to be a fundamental component of the hydrological cycle. It is also one of the least quantified, typically relying on empirical constitutive laws (e.g. Green et al. 2006). Fluid mechanics of transpiration involves coupled nonlinear flows in two adjacent media, a root system and an ambient soil (see the comprehensive reviews by Rand 1983; Passioura 1988; Green et al. 2006). These flows can be described by the Richards equation (e.g. Warrick 2003; Sperry et al. 2002),

$$\frac{\partial \theta}{\partial t} = -\nabla \cdot \mathbf{q}, \qquad \mathbf{q} = -\mathbf{K}(\psi)\nabla\Psi, \tag{1}$$

where $\theta \equiv \theta(\mathbf{x}, t)$ is the volumetric water content of a medium, $\mathbf{K} \equiv \mathbf{K}(\psi)$ is the hydraulic conductivity tensor, $\mathbf{q}(\mathbf{x}, t)$ is the macroscopic Darcy flux, $\Psi(\mathbf{x}, t)$ is the total hydraulic head, and a constitutive law (retention curve) relates the two state variables θ and Ψ. The hydraulic head of water in a soil, $\Psi = \psi + z$, consists of the pressure head (also known as matric potential or suction) $\psi = p_w/\gamma_w$ (with p_w and γ_w denoting the pressure and the specific weight of water, respectively) and the elevation head z. Pressure head in partially saturated media is less than atmospheric pressure head, i.e. $\psi < 0$.

In roots, the gradient of osmotic tension π can act as an additional force (Fiscus 1975), giving rise to $\Psi = \psi + z - \sigma\pi$ where σ is a reflection coefficient for solutes. However, it has long been argued (e.g. Fiscus 1975; Passioura 1988) that its influence during periods of active transpiration is negligible because soil water is usually diluted (Weatherley 1982). Following Roose and Fowler (2004a), Roose and Fowler (2004b), Schneider et al. (2010) and many others, we assume that $\sigma\pi \ll \psi + z$, i.e. define the total hydraulic head of water throughout a soil-root system as $\Psi = \psi + z$. This is appropriate for transpiration of low-salinity soil water (Green et al. 2006).

While a plethora of well-established constitutive laws and measurement techniques can be used to describe the pressure-dependent hydraulic conductivity of soils $K(\psi)$ (e.g. Warrick 2003), practical limitations of dealing with live plants render in situ determination of $K(\psi)$ for roots more problematic (Steudle 2000). Generally, the root conductivity depends on plant species, their age, and temperature (Lopez and Nobel 1991; Tsuda and Tyree 2000, and the references therein). Germane to this study is an experimental observation (ibid) that root conductivities decrease in drying soils, causing reduction in the water flux through a root.

Modern quantitative understanding of water uptake by roots dates back to 1950–60s mesoscopic models, which (1) treat a root as an infinite cylinder (of radius r_0) embedded in an infinite soil cylinder (of radius r_1, such that $r_0 \ll r_1$); (2) assume that flow from the soil into the root is strictly horizontal, i.e. employ the one-dimensional (in the radial direction) version of (1) to model flow in the soil shell $r_0 < r < r_1$; (3) suppose that the horizontal flow is driven by the difference in matric potentials

ψ_0 and ψ_1 at the boundaries $r = r_0$ and $r = r_1$, respectively; and (4) impose either a given flux (for constant rate of uptake) or a given saturation (for falling rate of uptake) at the root-soil interface $r = r_0$ (Raats 2007, and the references therein). A key finding of these models is that water uptake at both meso- and macro-scales is linearly proportional to the head difference $\Psi_1 - \Psi_0$ (Throughout this study we use Raat's definition of scales: "At the mesoscopic scale, uptake of water is represented by a flux at the soil-root interface, while at the macroscopic scale it is represented by a sink term in the volumetric mass balance."). This result underpins more sophisticated numerical models of plant transpiration and root water uptake (Roose and Fowler 2004a, b; Jong-van-Lier et al. 2006; Metselaar and Jong-van-Lier 2007; Javaux et al. 2008; Schneider et al. 2010; Couvreur et al. 2012).

We propose a root-scale analytical model, which either relaxes or eliminates the assumptions mentioned above. Instead of using an infinite cylinder to conceptualize a root, it imposes geometric and hydraulic constraints on its length. Our model does not postulate the existence of a soil cylinder with a known and spatially constant hydraulic head prescribed on its surface, and accounts for the vertical component of flow velocity in both the root and the soil. It uses measurable hydraulic quantities (infiltration rate and root-system suction) as input parameters, and enforces fundamental conservation laws at the root-soil interface. In Sect. 2, we formulate a mathematical model of water flow in soil-root systems and discuss its assumptions and limitations. In Sect. 3, we employ matched asymptotic expansions to derive an analytical solution to this problem. Its physical implications are discussed in Sect. 4. Salient features of our analysis are summarized in Sect. 5.

2 Problem formulation

2.1 Flow domain

A root system of a typical plant is geometrically complex, forming non-uniform branching networks. The analysis presented below explores kinematic underpinnings of the commonly used "cylindrical flow model" formulated as follows (Passioura 1988),

> "Despite the fact that root systems are branched, that the catchments of individual roots overlap in geometrically complicated ways, and that roots growing in real soil are typically not cylindrical because they must weave their ways past obstructions and often have to conform to the shapes of the pores within which they are growing, this model [water flowing radially towards a cylindrical, essentially isolated, root] remains useful. It can be extended to complete root systems, despite their complexity, by means of the simple but effective stratagem of imagining that each root has exclusive access to a cylinder of soil whose outer radius, R_{eff}, is half the average distance between roots. Radius R_{eff} can be calculated as $R_{\mathrm{eff}} = 1/\sqrt{\pi \rho_{\mathrm{av}}}$, where ρ_{av} is the average rooting density, the length of root in unit volume of soil."

From the outset, it is important to recognize that what Passioura (1988) and much of the subsequent literature on the subject call "the cylindrical flow model" refers not

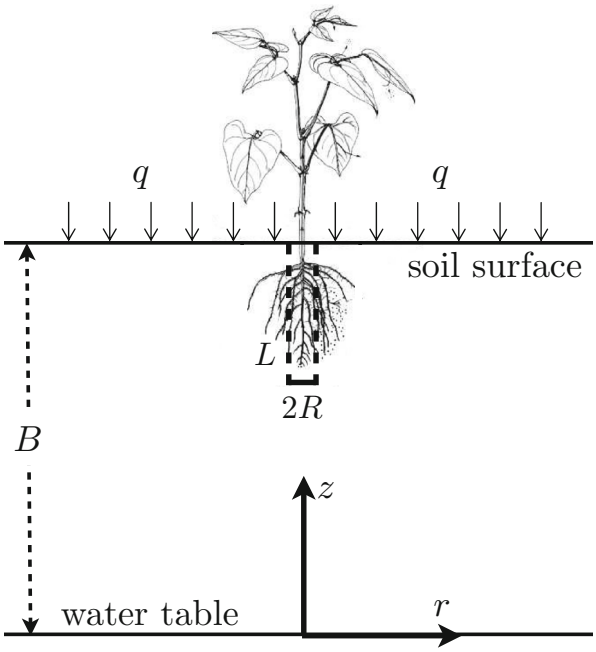

Fig. 1 Sketch of the water uptake induced by plant transpiration: a root system and its conceptualization with a single cylindrical root of radius R and length L. The vadose zone of thickness B separates the soil surface from the water table. Constant infiltration rate q is prescribed at the soil surface

only to root geometry but also to the flow configuration, in which water flows "radially in response to gradients in pressure, towards a cylindrical, essentially isolated, root".

We generalize the classical cylinder flow model by obviating the need for *a priori* restrictions on flow configuration in either the root system or the ambient soil. We consider a single root of radius R and length L in a homogeneous vadose zone (Fig. 1). The depth to groundwater, i.e. the thickness of a partially saturated soil (vadose zone), is denoted by B and assumed to be large enough for flow around the root to be unaffected by the water table. Finally, we assume axial symmetry and place the outer boundary of the flow domain at $r = R_{\text{eff}}$, such that $R_{\text{eff}} \gg R$ as defined in Passioura (1988). A baseline average rooting density $\rho_{\text{av}} = 1.0$ cm cm^{-3} (Passioura 1988) would result in the outer radius $R_{\text{eff}} \equiv 1/\sqrt{\pi \rho_{\text{av}}} \sim \mathcal{O}(1\,\text{cm})$. The resulting flow domain $\Omega = \{(r, z) : 0 \le r < R_{\text{eff}}, 0 \le z < B\}$ consists of two subdomains, $\Omega = \Omega_x \cup \Omega_s$ where $\Omega_x = \{(r, z) : 0 \le r < R, B - L \le z < B\}$ and $\Omega_s = \Omega / \Omega_x$ represent the root (xylem) and ambient soil, respectively. (Table 1 lists these and other symbols used in our analysis.)

2.2 Flow in ambient soil

Meteorological conditions that predominantly control transpiration rates vary rapidly in time, exhibiting marked diurnal fluctuations. Yet, a large number of studies reviewed

Table 1 Summary of the physical quantities and their dimensional counterparts

Symbol	Quantity	Units
(r, z)	Radial and vertical coordinates	L
B	Vadose zone thickness	L
L	Root length	L
R	Root radius	L
R_{eff}	External radius of the flow domain	L
ψ	Pressure head	L
ψ_0	Prescribed root suction at $z = B$	L
$\mathbf{q} = (q_r, q_z)^\top$	Macroscopic (Darcy) flux	L/T
q	Infiltration rate at soil surface	L/T
K_0 & K_x	Saturated hydraulic conductivities of xylem in the r and z Directions, respectively	L/T
K_s	Saturated hydraulic conductivity of ambient soil	L/T
α_x	Pore-size distribution parameter of xylem	1/L
α_s	Pore-size distribution parameter of ambient soil	1/L
Φ	Modified Kirchhoff transform of ψ	L
α	Step function equal to α_x in root and α_s in soil	1/L
$\kappa_r, \tilde{\kappa}_r, \kappa_z$ & $\tilde{\kappa}_z$	Conductivity ratios defined in (12b)	–
$\mathcal{K} = K_0/K_x$	Conductivity anisotropy ratio in xylem	–
$\chi = \alpha_s/\alpha_x$	Distribution parameter ratio	–
$\ell_r, \ell_z, \ell_\Phi$	Characteristic lengths defined in Sect. 3.2	–
$\varepsilon = (\ell_z/\ell_r)^2$	Small perturbation parameter	–
$\bar{A}$	Dimensionless counterparts of quantities $A = r, z, \ldots$	–
$(\tilde{r}, \tilde{z})$	Rescaled coordinates in boundary layer	–
$\mathcal{R} = \alpha_x R/2$	Scaled root radius	–
$J^\star$	Computed average transpiration flux	–

by Raats (2007) suggest that flow in both root systems and ambient soils can be represented by a sequence of steady states. This implies that a perturbation in the water potential ψ propagates instantaneously through a root zone. Cowan (1965), and the subsequent theoretical and experimental studies reviewed by Raats (2007), demonstrated that this approximation is adequate under typical conditions. Steady-state solutions are also used to interpret experimental data for water uptake by roots of various plants (Raats 2007, Sect. 4.5).

We therefore consider a steady-state ($\partial\theta/\partial t = 0$) version of (1) with $\Psi = \psi + z$,

$$\nabla \cdot [K_{\text{rel}}(\psi)\nabla\psi] + \frac{\partial}{\partial z} K_{\text{rel}}(\psi) = 0 \qquad (r, z) \in \Omega_s. \tag{2}$$

This formulation implies that the soil is homogeneous and isotropic, and represents its hydraulic conductivity $K(\psi) = K_s K_{\text{rel}}(\psi)$ as the product of (constant) saturated hydraulic conductivity K_s and the pressure-dependent relative hydraulic conductivity

$K_{\rm rel}(\psi)$. For the latter, we choose Gardner's model (e.g. Warrick 2003),

$$K_{\rm rel}(\psi) = \mathrm{e}^{\alpha_s \psi}, \tag{3}$$

where α_s is the pore-size distribution parameter. Due to its relative simplicity, the exponential model (3) is often used in both theoretical and experimental investigations of flow in partially saturated porous media. Tartakovsky et al. (2003a, 2004) provide an extensive list of studies that employ Gardner's model. Our choice of Gardner's model (3) facilitates the subsequent analytical treatment.

While more complicated constitutive relations, a plethora of which are compiled in Section 2.5 of Warrick (2003), often fit conductivity vs. saturation (or pressure head) data better, the reliance on the Gardner model is justified for the following reasons. First, using such constitutive relations (e.g. the Brooks-Corey or van Genuchten models) to fit sparse, spatially heterogeneous and error-prone data might not be warranted from the information-theory point of view. That is because these relations invariable rely on two or more fitting parameters, whereas Gardner's model (3) has only one. Second, the differences between the Gardner model and, say, the van Genuchten model are usually limited to saturation extremes corresponding to either nearly dry or nearly completely saturated soils, both of which detrimental to many plants. Third, the operational equivalency between various constitutive models $K_{\rm rel}(\psi)$ is achieved through their parameterization in a way that preserves the maximum value of macroscopic capillary length, which is defined as $H_c = \int_0^\infty K_{\rm rel}(s)\mathrm{d}s$ (e.g. Tartakovsky et al. 2003a). This quantity, which is also referred to as effective capillary drive, is directly related to the Kirchhoff transform used in the analysis below.

External boundary conditions for the Richards equation (3) are determined by physical processes at the soil surface ($z = B$) and water table ($z = 0$). Let q denote a prescribed (negative for infiltration) vertical Darcy flux at the soil surface $z = B$ (Fig. 1) due to rainfall or irrigation. This gives rise to a boundary condition

$$\mathrm{e}^{\alpha_s \psi}\left(1 + \frac{\partial \psi}{\partial z}\right) = -\frac{q}{K_s}, \qquad z = B, \quad R < r < R_{\rm eff}. \tag{4a}$$

The water table ($z = 0$) separates the (partially saturated) vadose zone where pressure head $\psi < 0$ from the (fully saturated) phreatic zone where $\psi > 0$. Hence, a boundary condition at the water table reads

$$\psi(r, 0) = 0, \qquad 0 \leqslant r < R_{\rm eff}. \tag{4b}$$

This formulation ignores (without loss of generality of the present analysis) the capillary fringe and sets atmospheric pressure head to $\psi_{\rm atm} = 0$. Finally, the external boundary $r = R_{\rm eff}$ is located sufficiently far from the root as to ensure that the latter does not affect the vertical flow (infiltration) in the rest of the soil ($r \geq R_{\rm eff}$). The corresponding boundary condition is

$$\frac{\partial \psi}{\partial r}(r = R_{\rm eff}, z) = 0, \qquad 0 \leq z \leq B. \tag{5}$$

2.3 Flow in root xylem

While soils might or might not be anisotropic, xylem's morphology renders its hydraulic conductivity anisotropic, with the longitudinal (along a root's length) saturated conductivity of xylem (K_x) being as much as seven orders of magnitude higher than its radial counterpart (K_0) (Sperry et al. 2002). The latter can be thought of as the harmonic mean of the low conductivities of inner and outer membranes, symplasm and xylem that comprise a root. Consequently, we treat the xylem hydraulic conductivity as a second-rank tensor,

$$\mathbf{K}(\psi) = \mathbf{K}_{\text{sat}} K_{\text{rel}}(\psi), \qquad \mathbf{K}_{\text{sat}} = \begin{pmatrix} K_0 & 0 \\ 0 & K_x \end{pmatrix}, \qquad K_{\text{rel}}(\psi) = \mathrm{e}^{\alpha_x \psi}. \quad (6)$$

Dependence of the xylem's relative conductivity K_{rel} on matric potential ψ arises due to cavitation; in this context, the function $K_{\text{rel}}(\psi)$ is referred to as a "vulnerability curve" (Sperry et al. 1998, 2002). Here, for the reasons described in the previous section, we adopted the Gardner model of $K_{\text{rel}}(\psi)$ with the pore-size distribution parameter of the root xylem denoted by α_x. Note that Gardner's model (3) is a special case of the Weibull distribution $K_{\text{rel}}(\psi) = \exp[-(-\alpha_x \psi)^c]$ used by Sperry et al. (1998) to represent vulnerability curves.

Finally, we use the steady-state Richards equation (1),

$$\nabla \cdot [\mathbf{K}(\psi) \nabla \psi] + K_x \frac{\partial}{\partial z} K_{\text{rel}}(\psi) = 0 \qquad (r, z) \in \Omega_x, \quad (7)$$

to describe flow in the root xylem.

Plant physiology suggests that no water uptake occurs at a root's end (Rand 1983; Passioura 1988). Thus, following Arbogast et al. (1993) and others, we impose a no-flow boundary condition at the root cylinder's bottom,

$$1 + \frac{\partial \psi}{\partial z} = 0 \qquad z = B - L, \quad 0 \le r < R. \quad (8)$$

A given pressure (suction) ψ_0 is prescribed at the soil surface, $z = B$, i.e. $\psi(r, B) = \psi_0$.

2.4 Coupling conditions at root-soil interface

Let R^- and R^+ denote the limit $r \to R$ from the root and soil sides of the interface $r = R$, respectively. Conservation of momentum and mass imposes continuity conditions on, respectively, pressure head ψ and the radial components of Darcy's flux q_r,

$$\psi(R^-, z) = \psi(R^+, z), \quad \left[K_r(\psi) \frac{\partial \psi}{\partial r} \right]_{r=R^-} = \left[K(\psi) \frac{\partial \psi}{\partial r} \right]_{r=R^+}, \quad B - L \le z \le B \quad (9)$$

where K_r is the radial component of the xylem conductivity tensor $\mathbf{K}$ given by (6).

These continuity conditions crystalize the difference between our "first-principle-based" approach and its empirical counterparts routinely used to model plant transpiration (e.g. Roose and Fowler 2004a, b; Green et al. 2006, and the references therein). Rather then enforcing the continuity of pressure across the root-soil interface $r = R$, the latter postulate the linear proportionality between the transpiration rate and the pressure (head) difference $\psi(R^+, z) - \psi(R^-, z)$. We defer a further discussion of this empirical approach to Sect. 4.

2.5 Integral transformation

We employ a modified Kirchhoff transformation,

$$\Phi(r, z) \equiv \mathrm{e}^{\alpha z/2} \int_{-\infty}^{\psi} K_{\mathrm{rel}}(s)\mathrm{d}s = \alpha^{-1}\mathrm{e}^{\alpha(\psi + z/2)}, \qquad \alpha = \begin{cases} \alpha_x & (r, z) \in \Omega_x \\ \alpha_s & (r, z) \in \Omega_s \end{cases}, \tag{10}$$

to map the Richards equations (2) and (7) onto their linear counterparts

$$\nabla^2\Phi - \frac{\alpha_s^2}{4}\Phi = 0, \qquad (r, z) \in \Omega_s \tag{11a}$$

and

$$\nabla \cdot (\mathbf{K}_{\mathrm{sat}} \nabla\Phi) - \frac{\alpha_x^2}{4} K_x \Phi = 0, \qquad (r, z) \in \Omega_x. \tag{11b}$$

The radial (q_r) and vertical (q_z) components of the volumetric flux $\mathbf{q} = (q_r, q_z)^\top$ defined in (1) are rewritten in terms of Φ as

$$\frac{q_r}{K_s} = -\tilde{\kappa}_r \mathrm{e}^{-\alpha z/2} \frac{\partial\Phi}{\partial r}, \qquad \frac{q_z}{K_s} = -\tilde{\kappa}_z \mathrm{e}^{-\alpha z/2} \left(\frac{\partial\Phi}{\partial z} + \frac{\alpha}{2}\Phi \right), \qquad (r, z) \in \Omega, \tag{12a}$$

where

$$\tilde{\kappa}_r = \begin{cases} \kappa_r = K_0/K_s & (r, z) \in \Omega_x \\ 1 & (r, z) \in \Omega_s \end{cases}, \qquad \tilde{\kappa}_z = \begin{cases} \kappa_z = K_x/K_s & (r, z) \in \Omega_x \\ 1 & (r, z) \in \Omega_s \end{cases}. \tag{12b}$$

The boundary conditions are transformed into

$$\mathrm{e}^{-\alpha_s B/2} \left[\frac{\partial\Phi}{\partial z} + \frac{\alpha_s}{2}\Phi \right]_{z=B} = -\frac{q}{K_s}, \qquad R < r < R_{\mathrm{eff}}; \tag{13}$$

$$\Phi(r, 0) = \alpha_s^{-1}, \quad 0 \le r < R_{\mathrm{eff}}; \qquad \frac{\partial\Phi}{\partial r}(r = R_{\mathrm{eff}}, z) = 0, \quad 0 \leqslant z \leqslant B; \tag{14}$$

and

$$\left[\frac{\partial\Phi}{\partial z}+\frac{\alpha_x}{2}\Phi\right]_{z=B-L}=0,\qquad \Phi(r,B)=\alpha_x^{-1}\mathrm{e}^{\alpha_x(\psi_0+B/2)},\qquad 0\le r\le R. \quad (15)$$

The continuity conditions (9) at the root-soil interface $\Gamma=\{(r,z): r=R,\, B-L\le z\le B\}$ take the form

$$(\alpha_x\Phi^-)^{\alpha_s}=(\alpha_s\Phi^+)^{\alpha_x},\quad \kappa_r\mathrm{e}^{-\alpha_x z/2}\left(\frac{\partial\Phi}{\partial r}\right)^-=-\mathrm{e}^{-\alpha_s z/2}\left(\frac{\partial\Phi}{\partial r}\right)^+, \quad (16)$$

where $\Phi^\pm\equiv\Phi(R^\pm,z)$ and $(\partial\Phi/\partial r)^\pm\equiv\partial\Phi/\partial r(R^\pm,z)$.

3 Perturbation solution

3.1 Dimensionless formulation

Both the identification of a small parameter and the subsequent perturbation analysis are facilitated by recasting the flow problem (11)–(16) in a dimensionless form. We introduce generic (as yet undefined) length scales ℓ_r, ℓ_z and ℓ_Φ to render dimensionless the coordinates and dependent variable,

$$\bar r=\frac{r}{\ell_r},\qquad \bar z=\frac{z}{\ell_z},\qquad \bar\Phi=\frac{\Phi}{\ell_\Phi}. \quad (17)$$

The Helmholtz equations (11) take a dimensionless form

$$\frac{(\ell_z/\ell_r)^2\mathcal{K}}{\bar r}\frac{\partial}{\partial\bar r}\left(\bar r\frac{\partial\bar\Phi}{\partial\bar r}\right)+\frac{\partial^2\bar\Phi}{\partial\bar z^2}-\frac{\bar\alpha^2}{4}\bar\Phi=0,\qquad \bar\alpha=\alpha\,\ell_z;\qquad (\bar r,\bar z)\in\bar\Omega \quad (18)$$

where $\mathcal{K}=K_0/K_x$ for $(\bar r,\bar z)\in\bar\Omega_x$ and $=1$ for $(\bar r,\bar z)\in\bar\Omega_s$. Here $\bar\Omega=\{(\bar r,\bar z): 0\le\bar r<\bar R_{\rm eff}, 0\le\bar z<\bar B\}$, and the transformed root and soil domains are defined respectively as $\bar\Omega_x=\{(\bar r,\bar z): 0\le\bar r<\bar R,\, \bar B-\bar L\le\bar z<\bar B\}$ and $\bar\Omega_s=\bar\Omega/\bar\Omega_x$, with $\bar R=R/\ell_r$, $\bar B=B/\ell_z$, $\bar L=L/\ell_z$ and $\bar R_{\rm eff}=R_{\rm eff}/\ell_r$. The boundary and continuity conditions (13)–(16) are transformed into

$$\frac{\ell_\Phi}{\ell_z}\frac{\partial\bar\Phi}{\partial\bar z}+\frac{\alpha\ell_\Phi}{2}\bar\Phi=\begin{cases}0 & \bar z=\bar B-\bar L,\quad 0<\bar r<\bar R\\ -\bar q\,\mathrm{e}^{\bar\alpha_s\bar B/2} & \bar z=\bar B,\quad \bar R<\bar r<\bar R_{\rm eff}\end{cases}; \quad (19)$$

$$\bar\Phi(\bar r,0)=\frac{1}{\alpha_s\ell_\Phi},\quad 0\le\bar r<\infty;\qquad \bar\Phi(\bar r,\bar B)=\frac{\mathrm{e}^{\bar\alpha_x(\bar\psi_0+\bar B/2)}}{\alpha_x\ell_\Phi},\quad 0\le\bar r\le\bar R; \quad (20)$$

and

$$(\alpha_x \ell_\Phi \bar{\Phi}^-)^\chi = \alpha_s \ell_\Phi \bar{\Phi}^+, \quad -\kappa_r \mathrm{e}^{-\bar{\alpha}_x \bar{z}/2} \left(\frac{\partial \bar{\Phi}}{\partial \bar{r}} \right)^- = \mathrm{e}^{-\bar{\alpha}_s \bar{z}/2} \left(\frac{\partial \bar{\Phi}}{\partial \bar{r}} \right)^+, \quad \bar{B} - \bar{L} \le \bar{z} \le \bar{B}; \tag{21}$$

where $\bar{q} = q/K_s$, $\bar{\psi}_0 = \psi_0/\ell_z$, and $\chi = \alpha_s/\alpha_x$. The dimensionless flux $\bar{\mathbf{q}} = (\bar{q}_r, \bar{q}_z)^\top$, with $\bar{q}_r = q_r/K_s$ and $\bar{q}_z = q_z/K_s$, is given by

$$\bar{q}_r = -\tilde{\kappa}_r \frac{\ell_\Phi}{\ell_r} \mathrm{e}^{-\bar{\alpha}\bar{z}/2} \frac{\partial \bar{\Phi}}{\partial \bar{r}}, \qquad \bar{q}_z = -\tilde{\kappa}_z \frac{\ell_\Phi}{\ell_z} \mathrm{e}^{-\bar{\alpha}\bar{z}/2} \left(\frac{\partial \bar{\Phi}}{\partial \bar{z}} + \frac{\bar{\alpha}}{2} \bar{\Phi} \right). \tag{22}$$

3.2 Characteristic length scales and small parameter identification

For thick vadose zones ($L \ll B$) considered in this study, the flow is characterized by four length scales: the root length (L) and radius (R), and the macroscopic capillary lengths of the root xylem (α_x^{-1}) and the ambient soil (α_s^{-1}). We identify a small parameter ε suitable for a perturbation analysis of (18)–(22) by relating ℓ_r, ℓ_z and ℓ_Φ in (17) to these four characteristic length scales as follows. In the root's absence, the flow (infiltration) would be vertical and described by the last two terms on the left-hand-side of (18). The root locally perturbs this background flow, introducing a radial dependence of the state variables in its vicinity. To account for this phenomenon, we define a small parameter in (18) as $\varepsilon \equiv (\ell_z/\ell_r)^2 \ll 1$, while requiring $\bar{\alpha} \equiv \alpha \ell_z \gg \varepsilon$. The same line of reasoning applied to the boundary conditions (19) and (20) suggests order relations $\ell_\Phi/\ell_z \gg \varepsilon$ and $\alpha \ell_\Phi \gg \varepsilon$. In summary, we require the generic length scales ℓ_r, ℓ_z and ℓ_Φ to satisfy inequalities

$$\left(\frac{\ell_z}{\ell_r} \right)^2 \equiv \varepsilon \ll 1, \qquad \varepsilon \ll \alpha \ell_\Phi, \qquad \varepsilon \ll \frac{\ell_\Phi}{\ell_z}, \qquad \varepsilon \ll \alpha \ell_z. \tag{23}$$

Selection of a set of the soil and root parameters L, R, α_s and α_x as the length scales ℓ_r, ℓ_z and ℓ_Φ is non-unique. It should be guided by site- and plant-specific values of these parameters and reflects a broad range of applicability of the perturbation solutions derived below. According to its definition in (10), the parameter α takes the values of α_x and α_s in Ω_s and Ω_x, respectively. A possible choice of the length scales that satisfies the order relations (23) is

$$\ell_z \equiv \alpha_s^{-1}, \qquad \ell_r \equiv R, \qquad \ell_\Phi \equiv L. \tag{24}$$

A number of productive soils exhibit the macroscopic capillary length $\alpha_s^{-1} = \mathcal{O}(10^{-1} \div 10\,\mathrm{cm})$ (Tartakovsky et al. 2003b, Fig. 1). Consider, as an example, mature main roots of grapevine (*Vitis vinifera* L.) with the ratio of $L/R = 42\,\mathrm{cm}/0.2\,\mathrm{cm}$ grown in a soil with $\alpha_s^{-1} = 10^{-1}\mathrm{cm}$. For these parameters, (23) and (24) yield $\varepsilon = 0.25$, $\alpha \ell_\Phi \sim \mathcal{O}(10^2)$, $\ell_\Phi/\ell_z = 420$ and $\alpha \ell_z \sim \mathcal{O}(1)$. A large variety of chaparral plants provide another pertinent example. According to Hellmers et al. (1955), largest roots

of California scrub oak (*Qifercuis duitnos* Nutt.) exhibit $R = 3.8$ cm and $L = 457$ cm. For the median range of capillary lengths, $\alpha_s^{-1} = \mathcal{O}(10^{-1} \div 1\text{cm})$, this results in $\varepsilon \sim 6.25 \times (10^{-6} \div 10^{-4})$, $\alpha\ell_\Phi \sim \mathcal{O}(10^2 \div 10^3)$, $\ell_\Phi/\ell_z \sim \mathcal{O}(10^2 \div 10^3)$ and $\alpha\ell_z \sim \mathcal{O}(1)$. Another set of the length scales is provided by (24) in which the last inequality is replaced by $\ell_\Phi \equiv \alpha_x^{-1}$. Thus the order relations (23) between the characteristic length scales account for a number of physical settings. In essence, our solution is valid for roots whose size is larger than the macroscopic capillary length of a host soil.

3.3 Outer solution

We look for a solution of (18)–(21) in the form of an asymptotic expansion in the small parameter ε,

$$\bar{\Phi}(\bar{r}, \bar{z}) = \sum_{k=0}^{\infty} \varepsilon^k \, \bar{\Phi}_k(\bar{r}, \bar{z}). \tag{25}$$

Boundary-value problems for $\bar{\Phi}_k(\bar{r}, \bar{z})$ are derived by substituting (25) into (18)–(21) and collecting the terms of k-th order in ε. In particular, the leading term in the expansion (25) satisfies

$$\frac{\partial^2 \bar{\Phi}_0}{\partial \bar{z}^2} - \frac{\bar{\alpha}^2}{4} \bar{\Phi}_0 = 0, \tag{26}$$

subject to the corresponding boundary conditions (19) and (20). This yields

$$\bar{\Phi}_0(\bar{z}) = \frac{\mathrm{e}^{-\bar{\alpha}\bar{z}/2}}{\alpha \, \ell_\Phi} \begin{cases} \mathrm{e}^{\bar{\alpha}_x(\bar{\psi}_0 + \bar{B})} & \text{in} \quad \bar{\Omega}_x \\ \\ 1 - \bar{q} \, (\mathrm{e}^{\bar{\alpha}_s \bar{z}} - 1) & \text{in} \quad \bar{\Omega}_s. \end{cases} \tag{27}$$

It follows from (22) and (27) that the zeroth-order approximation of the Darcian flux, $\bar{\mathbf{q}}_0 \equiv (\bar{q}_{r0}, \bar{q}_{z0})^\top$, has components

$$\bar{q}_{r_0} = 0, \qquad \bar{q}_{z_0} = \begin{cases} 0 & \text{in} \quad \bar{\Omega}_x \\ \\ \bar{q} & \text{in} \quad \bar{\Omega}_s. \end{cases} \tag{28}$$

The absence of derivatives with respect to $\bar{r}$ in the differential equation (26)—and the resulting lack of radial dependence of its solution (27)—implies that the continuity conditions (21) on the interface $\bar{r} = \bar{R}$ between $\bar{\Omega}_s$ and $\bar{\Omega}_x$ cannot be enforced. This indicates a singular nature of the asymptotic expansion (25), similar to that encountered in perturbation analyses of viscous flow past a sphere (e.g. Cohen and Kundu 2004), free-surface flow to a well (Dagan 1968), and transport of kinetically sorbing solutes in porous media (e.g. Severino et al. 2006).

Higher-order terms in the expansion (25) can be computed in an identical manner. Combined with their leading-order counterpart (27), they describe vertical flow in both the root ($\bar{\Omega}_x$) and the ambient soil ($\bar{\Omega}_s$) except in the regions adjacent to the boundary $\bar{r} = \bar{R}$ separating the two. We proceed to derive a solution for this boundary layer.

3.4 Inner (boundary-layer) solution

In the region adjacent to the root-soil interface $\bar{r} = \bar{R}$, the pressure ψ and its Kirchhoff transform Φ vary rapidly with the radius $\bar{r}$. The derivatives with respect to $\bar{r}$ in (18) become large enough that even multiplied by $\varepsilon \ll 1$ they cannot be neglected. To account for this behavior, we invoke the principle of the least degeneracy (Dyke 1975) to rescale the coordinates such that the leading-order term contains all the operator components that were neglected in the leading-order of the outer expansion. Within the boundary layer, we rescale the coordinates $(\bar{r}, \bar{z})$ as

$$\tilde{z} = \varepsilon^{1/4}\bar{z}, \qquad \tilde{r} = \varepsilon^{-1/2}\begin{cases} \bar{r} - \bar{R} & \text{for} \quad \bar{r} \geq \bar{R} \\ \bar{R} - \bar{r} & \text{for} \quad \bar{r} \leq \bar{R} \end{cases}. \tag{29}$$

Rewriting (18) in the $(\tilde{r}, \tilde{z})$ coordinates gives equations for $\bar{\Phi}$ in the boundary layer (denoted below by $\tilde{\Phi}$),

$$\frac{1}{\bar{R} + \sqrt{\varepsilon}\,\tilde{r}} \frac{\partial}{\partial \tilde{r}} \left[(\bar{R} + \sqrt{\varepsilon}\,\tilde{r}) \frac{\partial \tilde{\Phi}}{\partial \tilde{r}} \right] + \sqrt{\varepsilon} \frac{\partial^2 \tilde{\Phi}}{\partial \tilde{z}^2} - \frac{\bar{\alpha}_s^2}{4} \tilde{\Phi} = 0 \quad \text{in} \quad \tilde{\Omega}_s \tag{30a}$$

and

$$\frac{K_0/K_x}{\bar{R} - \sqrt{\varepsilon}\,\tilde{r}} \frac{\partial}{\partial \tilde{r}} \left[(\bar{R} - \sqrt{\varepsilon}\,\tilde{r}) \frac{\partial \tilde{\Phi}}{\partial \tilde{r}} \right] + \sqrt{\varepsilon} \frac{\partial^2 \tilde{\Phi}}{\partial \tilde{z}^2} - \frac{\bar{\alpha}_x^2}{4} \tilde{\Phi} = 0 \quad \text{in} \quad \tilde{\Omega}_x, \tag{30b}$$

where $\tilde{\Omega}_s$ and $\tilde{\Omega}_x$ are the regions of the boundary layer outside and inside the root, respectively. Equations (30) are subject to the continuity conditions (21).

Following Verhulst (2005), we introduce an auxiliary function

$$\phi(\tilde{r}, \tilde{z}) = \tilde{\Phi}(\tilde{r}, \tilde{z}) - \sum_{k=0}^{m} \varepsilon^k \bar{\Phi}_k(\tilde{z}), \tag{31}$$

where the last term represents the m-th order approximation of the outer expansion (25). This facilitates the subsequent matching of the inner and outer expansions by ensuring zero overlap between the inner and outer solutions. It follows from (18) that

$$\frac{\bar{\alpha}_s^2}{4} \bar{\Phi}_k - \sqrt{\varepsilon} \frac{\partial^2 \bar{\Phi}_k}{\partial \tilde{z}^2} \equiv \frac{\bar{\alpha}_s^2}{4} \bar{\Phi}_k - \frac{\partial^2 \bar{\Phi}_k}{\partial \bar{z}^2} = 0 \quad \text{for any} \quad k. \tag{32}$$

Hence, substituting (31) into (30) yields

$$\frac{1}{\bar{R}+\sqrt{\varepsilon}\,\tilde{r}}\,\frac{\partial}{\partial\tilde{r}}\left[(\bar{R}+\sqrt{\varepsilon}\,\tilde{r})\frac{\partial\phi}{\partial\tilde{r}}\right]+\sqrt{\varepsilon}\,\frac{\partial^2\phi}{\partial\tilde{z}^2}-\frac{\bar{\alpha}_s^2}{4}\,\phi=0 \quad \text{in} \quad \tilde{\Omega}_s \tag{33a}$$

and

$$\frac{K_0/K_x}{\bar{R}-\sqrt{\varepsilon}\,\tilde{r}}\,\frac{\partial}{\partial\tilde{r}}\left[(\bar{R}-\sqrt{\varepsilon}\,\tilde{r})\frac{\partial\phi}{\partial\tilde{r}}\right]+\sqrt{\varepsilon}\,\frac{\partial^2\phi}{\partial\tilde{z}^2}-\frac{\bar{\alpha}_x^2}{4}\phi=0 \quad \text{in} \quad \tilde{\Omega}_x. \tag{33b}$$

We look for a solution of (33) in the form of an asymptotic expansion

$$\phi(\tilde{r},\tilde{z})=\sum_{k=0}^{m}\varepsilon^{k/2}\,\phi_k(\tilde{r},\tilde{z})+\mathcal{O}(\varepsilon^{m+1/2}). \tag{34}$$

Substituting (34) into (33), using an expansion $(\bar{R}\pm\sqrt{\varepsilon}\,\tilde{r})^{-1}=1/\bar{R}\mp\sqrt{\varepsilon}\,\tilde{r}/\bar{R}^2+\mathcal{O}(\varepsilon)$, and collecting the terms of order ε^0, we obtain a leading-order equation

$$\mathcal{K}\frac{\partial^2\phi_0}{\partial\tilde{r}^2}-\frac{\bar{\alpha}^2}{4}\phi_0=0 \quad \text{in} \quad \tilde{\Omega}_s\cup\tilde{\Omega}_x. \tag{35}$$

Its general solution is

$$\phi_0(\tilde{r},\tilde{z})=c(\tilde{z})\,\mathrm{e}^{-\bar{\alpha}\tilde{r}/2\sqrt{\mathcal{K}}}+b(\tilde{z})\,\mathrm{e}^{\bar{\alpha}\tilde{r}/2\sqrt{\mathcal{K}}} \quad \text{in} \quad \tilde{\Omega}_s\cup\tilde{\Omega}_x \tag{36}$$

where $c(\tilde{z})$ and $b(\tilde{z})$ are "constants" of integration. For this expression to remain finite as $\varepsilon\to 0$, the definition of $\tilde{r}$ in (29) requires that $b(\tilde{z})\equiv 0$. Hence, it follows from (31) that

$$\tilde{\Phi}_0(\tilde{r},\tilde{z})=\bar{\Phi}_0(\tilde{z})+\mathrm{e}^{-\bar{\alpha}\tilde{r}/2\sqrt{\mathcal{K}}}\begin{cases}c_x(\tilde{z}) & \text{in} \quad \tilde{\Omega}_x\\ c_s(\tilde{z}) & \text{in} \quad \tilde{\Omega}_s\end{cases}. \tag{37}$$

The constants of integration $c_x(\tilde{z})$ and $c_s(\tilde{z})$ are determined from the continuity conditions (21) at the root-soil interface $\tilde{r}=0$, leading to

$$\tilde{\Phi}_0(\tilde{r},\tilde{z})=\bar{\Phi}_0(\tilde{z})+\frac{\xi(\tilde{z})}{\alpha\ell_\Phi}\,\exp\left[\frac{\bar{\alpha}}{2}\left(\frac{\tilde{z}}{\varepsilon^{1/4}}-\frac{\tilde{r}}{\sqrt{\mathcal{K}}}\right)\right]\begin{cases}K_s/\sqrt{K_0K_x} & \text{in} \quad \tilde{\Omega}_x\\ 1 & \text{in} \quad \tilde{\Omega}_s\end{cases} \tag{38}$$

where $\xi(\tilde{z})$ is a solution of the transcendental equation

$$\left[\frac{K_s\,\xi}{\sqrt{K_0K_x}}+\mathrm{e}^{\bar{\alpha}_x(\bar{\psi}_0+\bar{B}-\tilde{z}/\varepsilon^{1/4})}\right]^{\chi}=\xi+\mathrm{e}^{-\bar{\alpha}_s\tilde{z}/\varepsilon^{1/4}}-\bar{q}(1-\mathrm{e}^{-\bar{\alpha}_s\tilde{z}/\varepsilon^{1/4}}). \tag{39}$$

3.5 Matched asymptotic expansion and composite solution

According to Prandtl's limit matching principle (e.g. Dyke 1975, Ch. 5.7) $\bar{\Phi}^u$, a uniformly valid (composite) zeroth-order approximation of $\bar{\Phi}$, is obtained by summing up the corresponding inner ($\tilde{\Phi}_0$) and outer ($\bar{\Phi}_0$) solutions and subtracting their common part $\bar{\Phi}_{\rm com}$. Accounting for (38), this yields

$$\bar{\Phi}^u = -\bar{\Phi}_{\rm com} + 2\bar{\Phi}_0(\tilde{z}) + \frac{\xi}{\alpha \ell_\Phi} \exp\left[\frac{\bar{\alpha}}{2}\left(\frac{\tilde{z}}{\varepsilon^{1/4}} - \frac{\tilde{r}}{\sqrt{\mathcal{K}}}\right)\right] \begin{cases} K_s/\sqrt{K_0 K_x} & \text{in } \tilde{\Omega}_x \\ 1 & \text{in } \tilde{\Omega}_s \end{cases}. \tag{40}$$

Since far away from the root ($r \to \infty$) $\bar{\Phi}^u = \bar{\Phi}_0$, the common part $\bar{\Phi}_{\rm com} = \bar{\Phi}_0$. Thus, (40) and (27) give

$$\bar{\Phi}^u = \frac{1}{\alpha\, \ell_\Phi} \begin{cases} \mathrm{e}^{\bar{\alpha}_x(\bar{\psi}_0 + \bar{B} - \bar{z}/2)} + \dfrac{K_s \xi}{\sqrt{K_0 K_x}}\, \mathrm{e}^{-\alpha_x \ell_r (\bar{R} - \bar{r})/(2\sqrt{\mathcal{K}})} & \text{in } \bar{\Omega}_x \\ (1 + \bar{q})\, \mathrm{e}^{-\bar{\alpha}_s \bar{z}/2} - \bar{q}\, \mathrm{e}^{\bar{\alpha}_s \bar{z}/2} + \xi\, \mathrm{e}^{-\alpha_s \ell_r (\bar{r} - \bar{R})/(2\sqrt{\mathcal{K}})} & \text{in } \bar{\Omega}_s \end{cases}. \tag{41}$$

This expression for the normalized Kirchhoff transform, $\alpha_s \Phi^u \exp(-\alpha_s z/2)$, is plotted in Fig. 2 as a function of the dimensional radius $\alpha_s r$. It illustrates the boundary-layer behavior at the soil-root interface $\alpha_s R = 2.0$, for the parameter values reported in Table 2. Note that the boundary layer is wider in the root than in the soil. This is in

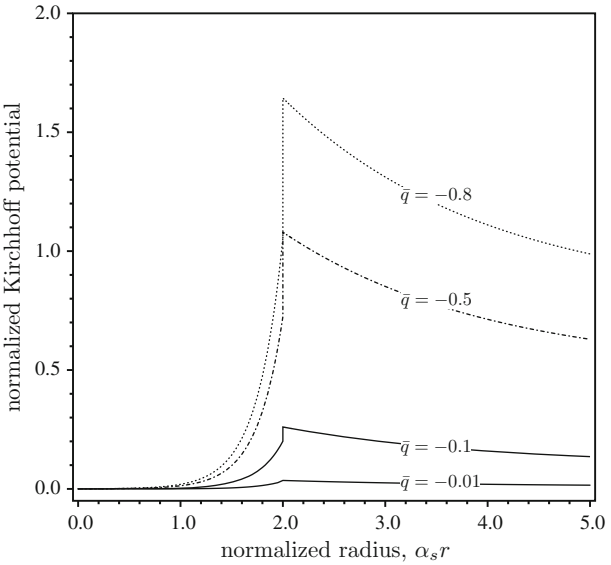

Fig. 2 Radial profiles of the normalized Kirchhoff potential $\alpha_s \Phi^u \exp(-\alpha_s z/2)$, for several values of the normalized infiltration rate $\bar{q} = q/K_s$. The root-soil interface is located at $\alpha_s R = 2.0$. The boundary layer around the interface, within which the Kirchhoff potential changes with r, is asymmetric. Its dimensionless width in the root is $\sim \mathcal{O}(\mathcal{K}\sqrt{\varepsilon})$, while that in the soil is $\sim \mathcal{O}(\sqrt{\varepsilon})$

Table 2 Parameter values used in the simulations

Parameter value	$\alpha_s = 10.0$	$K_s = 10.0$	$\alpha_x = 10^{-3}$	$K_x = 0.1$	$K_0 = 10^{-3}$	$R = 0.2$	$\psi_0 = -10^3$	$B = 10^3$
Units	cm^{-1}	cm/h	cm^{-1}	cm/h	cm/h	cm	cm	cm
Reference	Tartakovsky et al. (2003b)	Warrick (2003)	Miller (1985) and Philip (1968)	Sperry et al. (2002) and Frensch and Steudle (1989)	Sperry et al. (2002) and Frensch and Steudle (1989)	Doussan et al. (1998) and Mapfumo et al. (1994)	Allen et al. (1998)	–

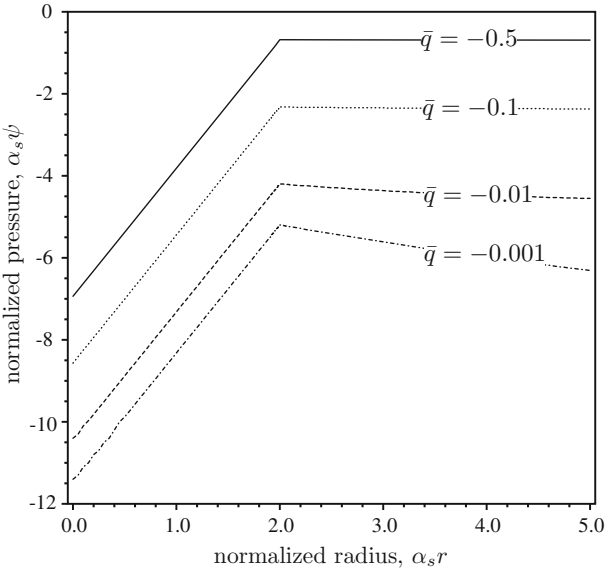

Fig. 3 Radial profiles of normalized pressure $\alpha_s\psi$, for several values of normalized infiltration rate $\bar{q} = q/K_s$. The root-soil interface is located at $\alpha_s R = 2.0$. Pressure ψ is maximum at the root-soil interface, from which it decays faster in the root than in the soil. Changes in infiltration rate q affect the pressure in the root more than in the soil

accordance with (38), which predicts that the widths of the boundary layer in the root and soil are $\mathcal{O}(\mathcal{K}\sqrt{\varepsilon})$ and $\mathcal{O}(\sqrt{\varepsilon})$, respectively.

Pressure distribution $\psi(\bar{r}, \bar{z})$ in the root-soil continuum is computed from (10) as $\alpha\,\psi = -\alpha\,z/2 + \ln(\alpha\,\ell_\Phi\bar{\Phi}^u)$. Its graphical representation in Fig. 3 reveals that the pressure ψ reaches its maximum value at the root-soil interface $r = R$, from which it decreases linearly inside the root ($r < R$) and monotonically outside the root ($r > R$). Away from the root ($r \gg R$) the pressure reaches its asymptotic value of $\alpha_s\psi_\infty = -\alpha_s z + \ln\left[1 - \bar{q}\,(\mathrm{e}^{\alpha_s z} - 1)\right]$. The pressure distribution predicted with (41), and depicted in Fig. 3, supports plant physiology studies [see e.g. Rand (1983), Passioura (1988)], which found that water suction (negative pressure) along the xylem is at least an order of magnitude higher than that in both the root-soil interface and the ambient soil.

The uniformly valid expression for the Darcian flux $\bar{\mathbf{q}}^u = (\bar{q}_r^u, \bar{q}_z^u)^\top$ is obtained by substituting (41) into (22),

$$\bar{q}_r^u(r,z) = \frac{\delta}{2}\,\xi\,\exp\left[-\frac{\delta\,\alpha}{2\sqrt{\mathcal{K}}}(r-R)\right], \quad \bar{q}_z^u(r,z) = \bar{q}_{z0} - \frac{2\,\delta}{\sqrt{\mathcal{K}}}\left(1 + \frac{\xi'}{\bar{\alpha}\,\xi}\right)\bar{q}_r^u(r,z), \tag{42}$$

where ξ' is the derivative of $\xi(\bar{z})$. The vertical component $\bar{q}_z^u$ approaches (exponentially) its far-field value of $\bar{q}_{z0}$ as r becomes large. This solution reflects the fact that far away from the root-soil interface the flux $\bar{\mathbf{q}}^u$ is vertical (Fig. 4). The radial com-

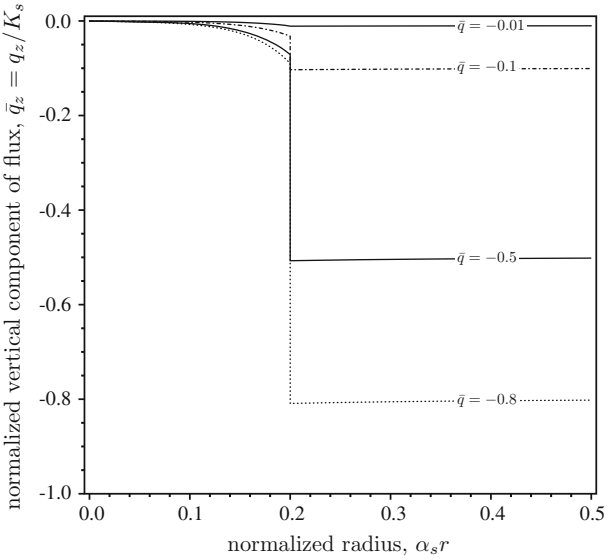

Fig. 4 Radial profiles of normalized vertical flux $\bar{q}_z = q_z/K_s$, for several values of normalized infiltration rate $\bar{q} = q/K_s$. The root-soil interface is located at $\alpha_s R = 2$. Outside the boundary layer, the vertical flux in the soil quickly reaches its far-field value $\bar{q}_{z0}$ as r increases

ponent $\bar{q}_r^u$ is non-zero only in the zone adjacent to the root-soil interface, decreasing exponentially with distance r (Fig. 5).

4 Results and discussion

The closed-form analytical solutions developed above enable us to derive from "first principles" two fundamental quantities of interest, plant's transpiration rate and root's capture zone. Unless specified otherwise, all the figures presented in this section correspond to the parameter values summarized in Table 2. They give rise to dimensionless parameters $\alpha_s B = -\alpha_s \psi_0 = 10^4$, $K_s/\sqrt{K_0 K_x} = 10^3$, $\alpha_s z = 9800$, $\alpha_s R = 2$, and $\mathcal{K} = 10^{-2}$.

4.1 Transpiration rate

For a root with circular cross-section $A = \pi R^2$, the Darcian flux in the root zone $q_z^u(r)$ and the plant transpiration rate Q_t are related by $Q_t = 2\pi \int_0^R |q_z^u(r)|\, r\, \mathrm{d}r$. The corresponding average transpiration flux $J^\star$ is defined as $J^\star = Q_t/(\pi R^2)$. Using the dimensional form of $q_z^u(r)$ in (42), we obtain

$$J^\star = 8\, K_s \left(\frac{K_0/K_x}{\alpha_x R}\right)^2 \left(\xi + \frac{\xi'}{\alpha_x}\right) \left[\frac{\alpha_x R}{2}\sqrt{\frac{K_x}{K_0}} + \exp\left(-\frac{\alpha_x R}{2}\sqrt{\frac{K_x}{K_0}}\right) - 1\right]. \quad (43)$$

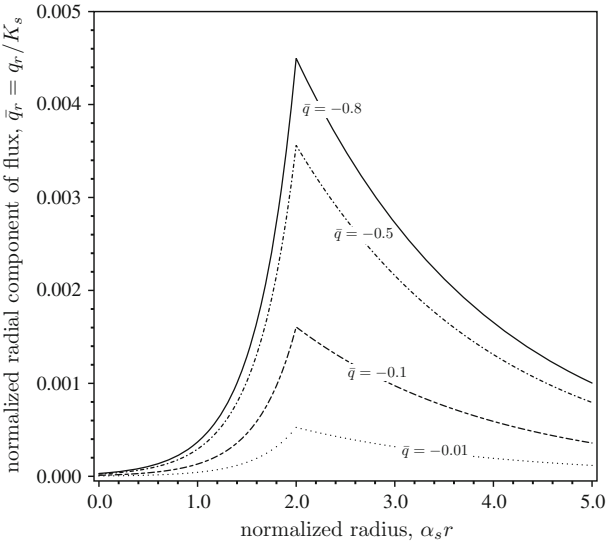

Fig. 5 Normalized radial flux $\bar{q}_r = q_r/K_s$ as a function of normalized radial distance $\alpha_s r$, for several values of normalized infiltration rate $\bar{q} = q/K_s$. The root-soil interface is located at $\alpha_s R = 2$. The radial flux is non-zero only in the boundary layer around the root-soil interface. Significant anisotropy of the root conductivity ($\mathcal{K} \ll 1$) is responsible for the asymmetry of the boundary layer within which q_r decays to zero (much faster in the root than in the soil)

To the best of our knowledge, (43) is the first closed-form analytical expression that relates plant transpiration to the soil (K_s and α_s) and root (K_0, K_x, α_x, and R) properties. It provides physical insight into the coupled nonlinear processes involved in root water uptake and, more generally, plant transpiration.

For a given set of hydraulic properties of the root xylem (K_0, K_x and α_x) and the soil (K_s and α_s), the average transpiration flux $J^\star$ (Fig. 6a) decreases, and the transpiration rate Q_t (Fig. 6b) increases, with the root radius R. While the former is in the dimensionless form that represents a wide range parameter combinations, the latter corresponds to the hydraulic properties specified in the beginning of this section. The values of Q_t in Fig. 6b are in line with the measurements (e.g. Steppe et al. 2005). The mean transpiration flux $J^\star$ is related to the pressure ψ at the center of the root. In particular, for $z = B$ the value $\psi^\star$ of the pressure determining the transpiration flux (43) is

$$\psi^\star = \alpha_x^{-1} \ln \left[\frac{K_s\, \xi(B)}{\sqrt{K_0 K_x}}\, \mathrm{e}^{-\mathcal{R}} + \mathrm{e}^{\alpha_x \psi_0} \right]. \tag{44}$$

These estimates of transpiration flux $J^\star$ and root suction $\psi^\star$ come with a caveat associated with the steady-state nature of our model (see the discussion in Sect. 2.2). While vadose zone processes are seldom stationary, the steady-state assumption is valid for precipitation or irrigation events leading to prolonged infiltration (e.g. Severino and Indelman 2004). As discussed in Sect. 2.2, steady-state solutions are building blocks in transient models that represent plant transpiration by a sequence of steady states. Moreover, in practice, plant transpiration rate is estimated by multiplying the maximum (i.e. steady-state) transpiration with a crop coefficient (Allen et al. 1998).

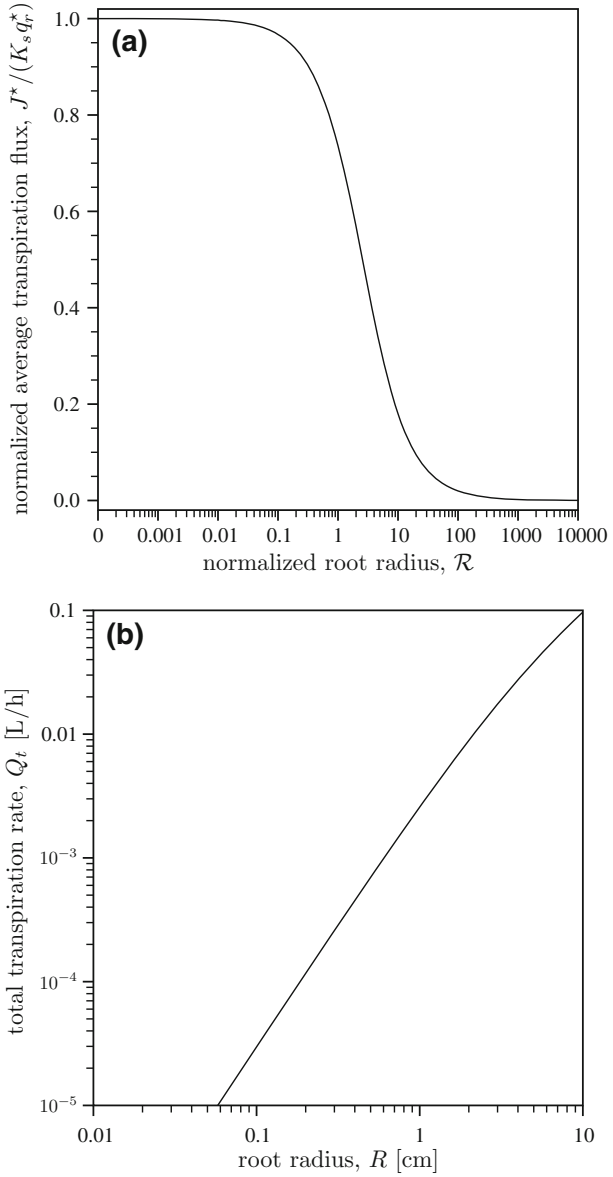

Fig. 6 **a** Average transpiration flux $J^\star$, normalized with $K_s q_r^\star = K_s(K_0/K_x)^2(\xi + \xi'/\alpha_x)$, as a function of the scaled root radius $\mathcal{R}$. Our model predicts that this relationship is a universal feature of water uptake by a single root, which is independent of the soil and root hydraulic properties. **b** Dependence of the transpiration rate Q_t on the root radius R for the parameter values listed in the Table 2

4.2 Capture zone

The soil region affected by a root's water uptake is referred to as a plant capture zone (PCZ). Estimating its size is essential for agriculture and phytoremediation, a process

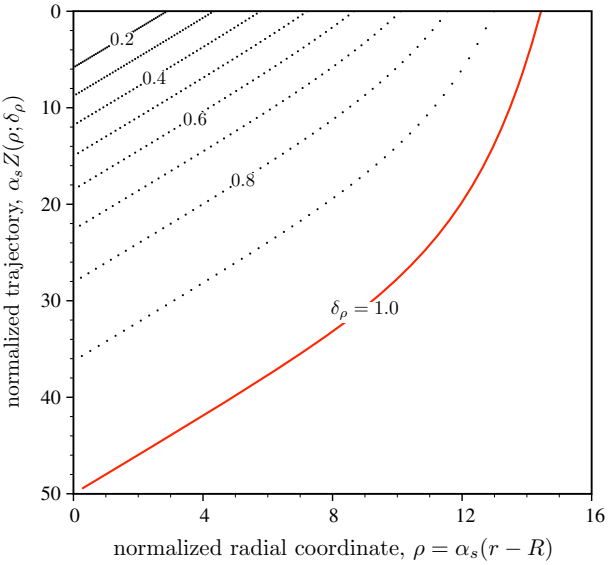

Fig. 7 Scaled trajectories $\alpha_s Z(r;\delta_\rho)$ of particles released on the soil surface at a relative distance δ_ρ from the root. The solid (red) line $\delta_\rho = 1.0$ delineates the plant capture zone (PCZ). Particles released on the soil surface at distance $r \le R_p^\star$ (or $\delta_\rho \le 1.0$) are captured by the root

in which plants are used to extract pollutants from contaminated soils. To delineate the PCZ, we compute a trajectory $Z = Z(r; R_p)$ of a particle released on the soil surface ($Z = B$) at a distance $r = R_p$ by solving numerically an ordinary differential equation

$$\frac{\mathrm{d}Z}{\mathrm{d}r} = \frac{q_z^u(r, Z)}{q_r^u(r, Z)}. \tag{45}$$

A trajectory bounding the PCZ originates on the soil surface at the critical distance $R_p^\star$, which is defined as a solution of $Z(0; R_p^\star) = L$ where L is the root's length.

Let $\rho = \alpha_s(r - R)$ denote the dimensionless radial coordinate that varies between the root ($r = R$) and a point $r = R_p > R$ on the soil surface at which a particle has been released. Let us define a dimensionless critical distance $\rho^\star = \alpha_s(R_p^\star - R)$ and introduce a maximum distance ratio $\delta_\rho = (R_p - R)/(R_p^\star - R)$. Trajectories $Z(\rho;\delta_\rho)$ with a label $\delta_\rho \le 1$ belong to the PCZ (Fig. 7). In other words, any particle released on the soil surface at distance $r \le R_p^\star$ will be captured by the root, while particles released at distance $r > R_p^\star$ will not.

Figure 8 reveals that the dimensionless critical distance $\rho^\star$ decreases monotonically with the normalized infiltration rate q/K_s. This is to be expected, since smaller infiltration values cause the root to draw water from larger volumes of the ambient soil. For the same reason, $\rho^\star$ increases with the dimensionless root length $\alpha_s L$.

Combined with the definition of dimensionless critical distance $\rho^\star$, Fig. 8 suggests that for a given infiltration rate q a root in a soil with larger saturated conductivity K_s and/or the Gardner parameter α_s would have a larger capture zone (i.e. larger $\rho^\star$ or

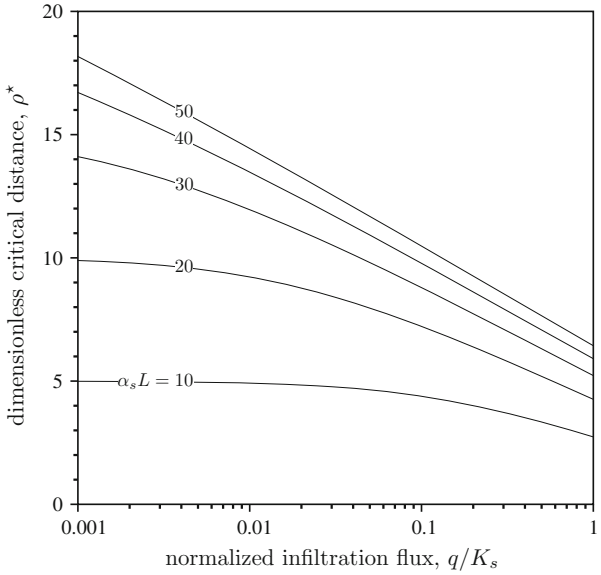

Fig. 8 Dependence of the critical distance of the plant capture zone, $\rho^\star$, on infiltrating rate q/K_s, for several values of scaled root length $\alpha_s L$. The critical distance defines the maximum radial extent of the capture zone. The monotonic decrease of $\rho^\star$ with q/K_s indicates that smaller infiltration values cause the root to draw water from larger volumes of the ambient soil. For the same reason, $\rho^\star$ increases with the dimensionless root length $\alpha_s L$

$R_p^\star$). Larger values of K_s result in larger values of vertical flux q_z, thus enhancing the vertical infiltration and hence reducing the amount of water available for root water uptake. Large values of α_s have a similar effect. They represent soils with reduced soil-water retention, which are conducive to gravity-driven (vertical) flows (Philip 1968), once again reducing the amount of water available for root water uptake and causing the root to "interrogate" large volumes of the ambient soil. Finally, Fig. 8 suggests that, for given soil and root parameters, roots with larger lengths L have larger $\rho^\star$ and hence capture zones.

4.3 Comparison with empirical models of plant transpiration

Our root-scale model of water uptake is based on first principles, i.e. employs the generally accepted Richards equation to describe water flow in partially saturated porous media (both in a root and the ambient soil) and makes no assumptions about the kinematic structure of flow in a root-soil continuum. That is in contrast with the existing root-scale (Type I) and mesoscale (Type II) models (Green et al. 2006; Raats 2007): the former impose *a priori* constraints on the kinematic structure of flow, such as the assumptions (ii)–(iv) discussed in the Introduction; and the latter are entirely empirical. The classification of root water uptake models into Types I and II is due to Green et al. (2006).

Our analytical solution (see Sect. 3.4) provides a theoretical justification for several assumptions that underpin the existing Type I models. Specifically, it demonstrates

that flow is strictly horizontal (perpendicular to the root) in the boundary layer on both side of the soil-root interface. This provides a theoretical justification for empirical infinite-soil-cylinder mesoscopic models (Raats 2007, and the references therein) . They *assume* that flow is horizontal and driven by the difference in matric potentials ψ_0 and ψ_1 imposed at the surfaces of the soil shell $R < r < r_1$, where r_1 is an arbitrarily assigned external radius of the soil cylinder. Our solution suggests that the radius r_1 of such soil cylinders is given by the boundary layer thickness ϵ. The latter varies with the root geometry and/or hydraulic properties of the root and the ambient soil, as discussed in Sect. 3.2.

5 Summary and concluding remarks

We derived, from first principles, a closed-form analytical solution for plant transpiration, i.e. for flow of water from the partially saturated ambient soil to a plant's root. The underlying model consists of two three-dimensional Richards' equations that are coupled at the root-soil interface. The root is conceptualized as a cylinder of length L and radius R. The system behavior is controlled by vertical and horizontal length scales ℓ_z and ℓ_r. For a wide range of natural conditions, $\varepsilon = (\ell_z/\ell_r)^2 \ll 1$ and serves as a perturbation parameter.

A matched asymptotic expansion technique was used to derive approximate solutions for transpiration rate and the size of a plant capture zone (PCZ). To the best of our knowledge, this is the first closed-form analytical expression that relates a plant's transpiration rate to the soil and root hydraulic properties by relying on first principles, rather than phenomenology. As such, it sheds new light on plant transpiration, one of the least-understood components of the hydrological cycle.

Our analysis leads to the following major conclusions.

- Away from the root-soil interface the water flux $\mathbf{q}$ is vertical. The radial component of $\mathbf{q}$ is non-zero only within the boundary layer adjacent to the root-soil interface. This provides a theoretical justification for the currently used empirical "infinite soil cylinder" mesoscopic models.
- The radial component of $\mathbf{q}$ decays exponentially with the radial distance from the soil-root interface as consequence of the rapid variation due to the boundary-layer transitional effect.
- The PCZ size increases as the infiltration rate decreases relative to the radial flux at the soil-root interface.

Several assumptions underpin the presented model (see Sect. 2). Some of them can be relaxed or altogether eliminated within our analytical framework. ◇ The assumption of soil homogeneity was used to treat soil hydraulic properties as constants. It can be relaxed by assuming that a soil is statistically homogeneous (i.e. its parameters have constant ensemble means and variances) and employing stochastic homogenization (Tartakovsky et al. 2003a, b). ◇ The steady-state assumption can be eliminated by adopting an exponential pressure (ψ) vs. saturation (θ) constitutive law, $\theta \sim \exp(\alpha_s \psi)$. This would allow one to account for transient flow regimes, while retaining the ability to linearize the Richards equation by deploying the Kirchhoff transformation (Tartakovsky et al. 2004). ◇ Finally, our model represents a root system

with a single cylinder. It can serve as a building block in more realistic models (Roose and Fowler 2004a), which represent root networks as branching systems of cylinders. These generalizations are the focus of our ongoing studies.

Acknowledgments This research was supported in part by the National Science Foundation award EAR-1246315 and by the Computational Mathematics Program of the Air Force Office of Scientific Research. The first author acknowledges support from "Programma di scambi internazionali per mobilitá di breve durata" (Naples University, Italy), "OECD Cooperative Research Programme: Biological Resource Management for Sustainable Agricultural Systems" (Contract No. JA00073336), and PRIN project "I paesaggi tradizionali dell'agricoltura italiana: definizione di un modello interpretativo multidisciplinare e multiscala finalizzato alla pianificazione e alla gestione" (Contract No. 2010LE4NBM_007). The first author thanks Prof. Gerardo Toraldo (Naples University) for promoting his visit to University of California, San Diego; and Dr. Peng Wang for his kind hospitality.

References

Allen RG, Pereira LS, Raes D, Smith M (1998) Crop evapotranspiration—guidelines for computing crop water requirements. In: Technical Report FAO Irrigation and drainage paper 56, ISBN 92-5-104219-5, FAO—food and agriculture organization of the united nations

Alm DM, Cavelier J, Nobel PS (1992) A finite element method of radial and axial conductivitives for individual roots: development and validation for two desert succulents. Ann Bot 69:87–92

Arbogast T, Obeyesekere M, Wheeler MF (1993) Numerical methods for the simulation of flow in root-soil systems. SIAM J Numer Anal 30:1677–1702

Caldwell MM, Richars JH (1986) Competing root systems: morphology and models of absorption. In: Civnish TJ (ed) On the economy of plant form and function. Cambridge University Press, Cambridge, pp 251–273

Carminati A, Moradi AB, Vetterlein D, Weller U, Vogel H-J, Oswald SE (2010) Dynamics of soil water content in the rhizosphere. Plant Soil 332(1–2):163–176

Cohen IM, Kundu PK (2004) Fluid mechanics. Elsevier, New York

Cole JD (1968) Perturbation methods in applied mathematics. Blaisdell, New York

Couvreur V, Vanderborght J, Javaux M (2012) A simple three-dimensional macroscopic root water uptake model based on the hydraulic architecture approach. Hydrol Earth Syst Sci

Cowan IR (1965) Transport of water in the soil-plant-atmosphere system. J Appl Ecol 2:221–239

Dagan G (1968) A derivation of Dupuit solution of steady flow toward wells by matched asymptotic expansions. Water Resour Res 4:403–412

Dagan G (1971) Perturbation solutions of the dispersion equation in porous mediums. Water Resour Res 7:135–142

Day SD, Wiseman PE, Dickinson SB, Harris JR (2010) Contemporary concepts of root system architecture of urban trees. Arboric Urban For 36(4):149–159

De Jong-van-Lier Q, Metselaar K, van Dam JC (2006) Root water extraction and limiting soil hydraulic conditions estimated by numerical simulation. Vadose Zone J 5:1264–1277

Doussan C, Pages L, Vercambre G (1998) Modelling of the hydraulic architecture of root systems: an integrated approach to water absorption-model description. Ann Botany 81:213–223

De Willigen P, Van Noordwijk M (1994a) Mass flow and diffusion of nutrients to a root with constant or zero-sink uptake 1. Constant uptake. Soil Sci 157:162–170

De Willigen P, Van Noordwijk M (1994b) Mass flow and diffusion of nutrients to a root with constant or zero-sink uptake 2. Zero-sink uptake. Soil Sci 157:171–175

Fiscus EL (1975) The interaction between osmotic and pressure-induced water flow in plant roots. Plant Physiol 59:1013–1020

Frensch J, Steudle E (1989) Axial and radial hydraulic resistance to roots of maize *Zea mays* L. Plant Physiol 91:719–726

Green SR, Kirkham MB, Clothier BE (2006) Root uptake and transpiration: from measurements and models to sustainable irrigation. Agric Water Manage 86:165–176

Hellmers H, Horton JS, Juhren G, O'Keefe J (1955) Root systems of some chaparral plants in southern California. Ecology 36(4):667–678

Hinsinger P, Gobran GR, Gregory PJ, Wenzel WW (2005) Rhizosphere geometry and heterogeneity arising from root-mediated physical and chemical processes. New Phytol 168:293–303
Javaux M, Schröder T, Vanderborght J, Vereecken H (2008) Use of a three-dimensional detailed modeling approach for predicting root water uptake. Vadose Zone J 7:1079–1088
Linton MJ, Nobel PS (2001) Hydraulic conductivity, xylem cavitation, and water potential for succulent leaves of *Agave deserti* and *Agave tequilana*. J Plant Sci 162:747–754
Lopez FB, Nobel PS (1991) Root hydraulic conductivity of two cactus species in relation to root age, temperature, and soil water status. J Exp Botany 42:143–149
Mapfumo E, Aspinall D, Hancock TW (1994) Growth and development of roots of grapevine (*Vitis vinifera* L.) in relation to water uptake from soil. Ann Botany 74(1):75–85
Metselaar K, de Jong-van-Lier Q (2007) The shape of the transpiration reduction function under plant water stress. Vadose Zone J 6:124–139
Miller EC (1916) Comparative study of the root systems and leaf areas of corn and the sorghums. J Agric Res 6(9):311–331
Miller DM (1985) Studies of root function in Zea mays. Plant Physiol 77:168–174
Passioura JB (1988) Water transport in and to roots. Ann Rev Plant Physiol Plant Mol Biol 39:245–265
Philip JR (1968) Steady infiltration from buried point sources and spherical cavities. Water Resour Res 4(5):1039–1047
Philip JR (1989) The scattering analog for infiltration in porous media. Rev Geophys 27(4):431–448
Pinder GF, Celia MA (2006) Subsurface hydrology. Wiley, New York
Raats PAC (2007) Uptake of water from soils by plant roots. Transp Porous Media 68:5–28
Rand RH (1983) Fluid mechanics of green plants. Ann Rev Fluid Mech 15:29–45
Roose T, Fowler AC (2004a) A mathematical model for water and nutrient uptake by plant root systems. J Theor Biol 228:173–184
Roose T, Fowler AC (2004b) A model for water uptake by plant roots. J Theor Biol 228:155–171
Schneider CL, Attinger S, Delfs J-O, Hildebrandt A (2010) Implementing small scale processes at the soil-plant interface—the role of root architectures for calculating root water uptake profiles. Hydrol Earth Syst Sci 14:279–289
Severino G, Indelman P (2004) Analytical solutions for reactive solute transport under an infiltration–redistribution cycle. J Contam Hydrol 70:89–115
Severino G, Monetti VM, Santini A, Toraldo G (2006) Unsaturated transport with linear kinetic sorption under unsteady vertical flow. Transp Porous Media 63:147–174
Smith DM, Meinzer FC, Allen SJ (1996) Measurement of sap flow in plant stems. J Exp Bot 47(305):1833–1844
Sperry JS, Adler FR, Campbell GS, Comstock JP (1998) Limitation of plant water use by rhizosphere and xylem conductance: results from a model. Plant Cell Environ 21(4):347–359
Sperry JS, Hacke UG, Oren R, Comstock JP (2002) Water deficits and hydraulic limits to leaf water supply. Plant Cell Environ 25:251–263
Steppe K, De Pauw D, Lemeur R, Vanrolleghem PA (2005) A mathematical model linking tree sap flow dynamics to daily stem diameter fluctuations and radial stem growth. Tree Physiol 26:257–273
Steudle E (2000) Water uptake by roots: effects of water deficit. J Exp Botany 51:1531–1542
Tartakovsky DM, Guadagnini A, Riva M (2003a) Stochastic averaging of nonlinear flows in heterogeneous porous media. J Fluid Mech 492:47–62
Tartakovsky DM, Lu Z, Guadagnini A, Tartakovsky AM (2003b) Unsaturated flow in heterogeneous soils with spatially distributed uncertain hydraulic parameters. J Hydrol 275(3–4):182–193
Tartakovsky AM, Garcia-Naranjo L, Tartakovsky DM (2004) Transient flow in a heterogeneous vadose zone with uncertain parameters. Vadose Zone J 3(1):154–163
Tsuda M, Tyree MT (2000) Plant hydraulic conductance measured by the high pressure flow meter in crop plants. J Exp Botany 345:823–828
van Dyke MD (1975) Perturbation methods in fluid mechanics. Academic Press, New York
Verhulst F (2005) Methods and applications of singular perturbation. Springer, New York
Wallach R (1998) A small perturbations solution for nonequilibrium chemical transport through soils with relatively high desorption rate. Water Resour Res 34:149–154
Warrick AW (2003) Soil water dynamics. Oxford University Press, Oxford
Weatherley PE (1982) Water uptake and flow in roots. In: Lange OL, Nobel PS, Osmond CB, Ziegler H (eds) Physiological plant ecology—II water relations and carbon assimilation. Springer, New York, pp 79–109